Available online at www.sciencedirect.com
ScienceDirect
Applied Surface Science 253 (2006) 2078–2086
applied surface science
www.elsevier.com/locate/apsusc

Stabilization of discotic liquid organic thin films by ITO surface treatment

S. Archambeau [a], I. Séguy [a], P. Jolinat [a], J. Farenc [a], P. Destruel [a,*], T.P. Nguyen [b], H. Bock [c], E. Grelet [c]

[a] *Laboratoire de Génie Electrique de Toulouse, Université Paul Sabatier, 31062 Toulouse Cedex 09, France*
[b] *Institut des Matériaux Jean Rouxel, CNRS, Université de Nantes, 44322 Nantes, France*
[c] *Centre de Recherche Paul Pascal, CNRS, Université Bordeaux 1, 33600 Pessac, France*

Received 6 March 2006; received in revised form 29 March 2006; accepted 2 April 2006
Available online 22 May 2006

Abstract

Discotic liquid crystals (LCs) are promising materials in the field of electronic components and, in particular, to make efficient photovoltaic cells due to their good charge transport properties. These materials generally exhibit a mesophase in which the disk-shaped molecules can self-assemble into columns, which favorize charge displacement, and may align themselves uniformly on surfaces to form well-oriented thin films. In order to orientate such a columnar thin film on an indium tin oxide (ITO) substrate, the film is heated up to the temperature range of the isotropic liquid phase and subsequently cooled down again. This treatment may lead not only to the desired alignment, but also to dewetting, which leads to an appreciable inhomogeneity in film thickness and to short circuits during the realization of photovoltaic cells. In this article, we describe how this dewetting and the film morphology can be influenced by ITO surface treatments. The chemical modifications of the surface by these treatments were studied by X-ray photoelectron spectroscopy (XPS). Such ITO treatments are shown to be efficient to prevent thin film dewetting when combined with rapid cooling through the isotropic-to-LC phase transition.

PACS: 61.30 Hn; 68.35 Fx; 61.30 −v; 68.55.−a; 79.60 Fr; 81.15.−z

Keywords: Discotic liquid crystal; Dewetting; ITO treatments; XPS

1. Introduction

Organic charge transport materials currently attract considerable interest due to their potential use in organic electronic and optoelectronic devices such as organic field effect transistors (OFETs) and plastic solar cells (PSCs) [1–4]. Organic ''semiconductors'' exhibit charge mobilities and exciton diffusion lengths that are orders of magnitude smaller than inorganic semiconductors such as polycrystalline silicon [1,2] and considerable research efforts are focused on the improvement of these parameters by appropriate self-assembly of electronically active organic materials into ordered and well-conducting structures. Such structures include epitaxially grown single crystals [3], interdigitated heterojunctions [4] and oriented liquid crystalline domains [5].

Our research interests are focused in particular on columnar liquid crystals, whose excellent one-dimensional charge transport properties within well-oriented domains [6–9] make them good candidates for organic electronic devices if an appropriate orientation of the axis of preferred transport is obtained by control of the domain growth. The preferred orientation of the column axis depends on the type of device. For instance, field effect transistors require planar (parallel) alignment of the columns with the substrate surface, while solar cells require homeotropic (perpendicular) alignment of the columns on the substrate.

One straightforward approach to well-aligned columnar thin films is based on the annealing of the initially disordered organic layer by heating it up above the liquid crystal—isotropic liquid transition (at the ''clearing'' temperature) and

* Corresponding author. Tel.: +33 561 55 62 61; fax: +33 561 55 64 52.
E-mail address: pierre.destruel@lget.ups-tlse.fr (P. Destruel).

0169-4332/$ – see front matter © 2006 Elsevier B.V. All rights reserved.
doi:10.1016/j.apsusc.2006.04.004

then cooling down with a controlled rate through the transition to obtain large, well-aligned domains. The alignment obtained may be planar or homeotropic, depending on the material, on the substrate and on the conditions chosen (film thickness and cooling rate) [10].

Several criteria have to be met by the organic film and the material used for obtaining its alignment by annealing:

(1) The material has to exhibit a clearing transition within the available temperature range.
(2) The material must be chemically stable at and slightly above this temperature.
(3) The material needs to wet the substrate both in its isotropic liquid state and in its columnar liquid crystalline phase.

We have in recent years developed a class of electronically active and thermally stable columnar liquid crystalline materials with different aromatic chromophores: the alkyl esters of arene-oligocarboxylic acids. These materials exhibit a columnar liquid crystalline phase at or near room temperature and show accessible clearing temperatures. We have obtained both organic light emitting diodes [11] and solar cells [9] based on such esters and closely related imido-esters. Perylene tetracarboxylic alkyl esters are particularly easily accessible in large quantities, as their synthesis from perylene-3,4,9,10-tetracarboxylic dianhydride (PTCDA) requires only a single esterification step.

While criteria (1) and (2) are met by such materials, criteria (3), the wetting of the film during annealing on typical electrode substrates such as commercial ITO-coated glass, is often not obtained in very thin (<100 nm) films which are required for organic solar cells, light emitting diodes and field effect transistors, without any particular substrate treatment. If the film thickness is below a critical value, typically of several hundred nanometers, the initial spin-coated or vacuum deposited film, which consists of domains of random orientation and few microns in diameter, clears to an isotropic liquid that rapidly destabilizes into isolated droplets. To avoid this droplet formation and to stabilize a continuous liquid film of uniform thickness from which large columnar domains may be grown on cooling, we have studied the influence of various surface treatments on the wetting behavior of perylene ester in the isotropic liquid state (above 210 °C; see Fig. 1). As no significant difference in dewetting behavior is observed on glass, gold, silicon or ITO surfaces, we focus on ITO substrates in this study because ITO is the commonly chosen transparent anode material for organic solar cells and light emitting diodes.

2. Materials and methods

Perylene-3,4,9,10-tetracarboxylic tetrapentyl ester was synthesized by esterification of PTCDA with pentanol and 1-bromopentane in the presence of potassium carbonate [12].

ITO thin films deposited on glass substrates were purchased from TFD (Thin Film Devices, USA). Their thickness and their sheet resistance were, respectively, 130 nm and 15 Ω/□. All ITO coated glass substrates were immersed in an ultrasonic

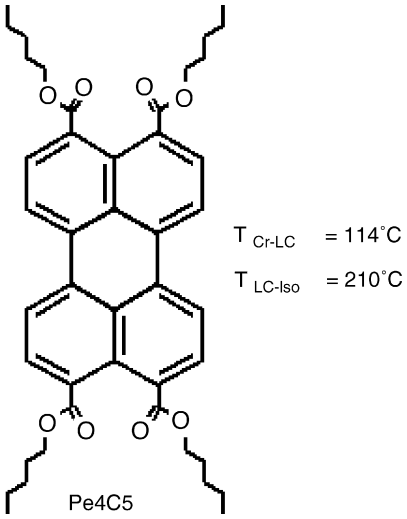

Fig. 1. Molecular structure of the liquid crystalline material, with phase transition temperatures.

methanol bath for 15 min, rinsed with deionized water and dried under nitrogen flow. ITO surfaces only cleaned by this procedure, without further treatment, are called ''untreated'' throughout this manuscript.

The organic films were deposited by vacuum evaporation at a pressure of 10^{-6} mbar on ITO. The chemicals were placed in flat silica cupels located 25 cm below the substrate. The deposition rate of the evaporated materials (~1 Å/s) and the thickness of each layer were controlled by a quartz vibrating thickness monitor placed near the samples. The LC layers were heated in a heating stage placed under a standard polarizing microscope (Zeiss). The heating and cooling rates were typically 10 °C/min. Thin film roughness and thickness measurements were performed with a Tenkor mechanical profilometer.

XPS measurements were carried out on a Leybold LHS-12 spectrometer (CNRS-Université de Nantes), using a magnesium cathode ($h\nu$ = 1253.6 eV), operating at 12 kV and 10 mA. The energy pass was set at 25 eV for all the experiments. The pressure of the chamber was kept around 10^{-9} mbar. The recorded spectra were corrected with satellite and Shirley background subtractions. Gaussian and Lorentzian function combinations were used by varying parameters such as Gaussian/Lorentzian ratio, full width at half maximum (FWHM), intensity and position of each contribution to obtain the best fit of the experimental curves. Determination of the atomic concentrations of the film surface was performed using the atomic sensitivity factors supplied by Leybold software.

3. Results

Tetrapentyl perylene-3,4,9,10-tetracarboxylate exhibits its hexagonal columnar liquid crystalline mesophase between its melting point at 114 °C and its clearing transition to the isotropic liquid at 210 °C.

Thin films (50 nm) deposited on ITO substrates were heated above the clearing transition and then cooled down. No

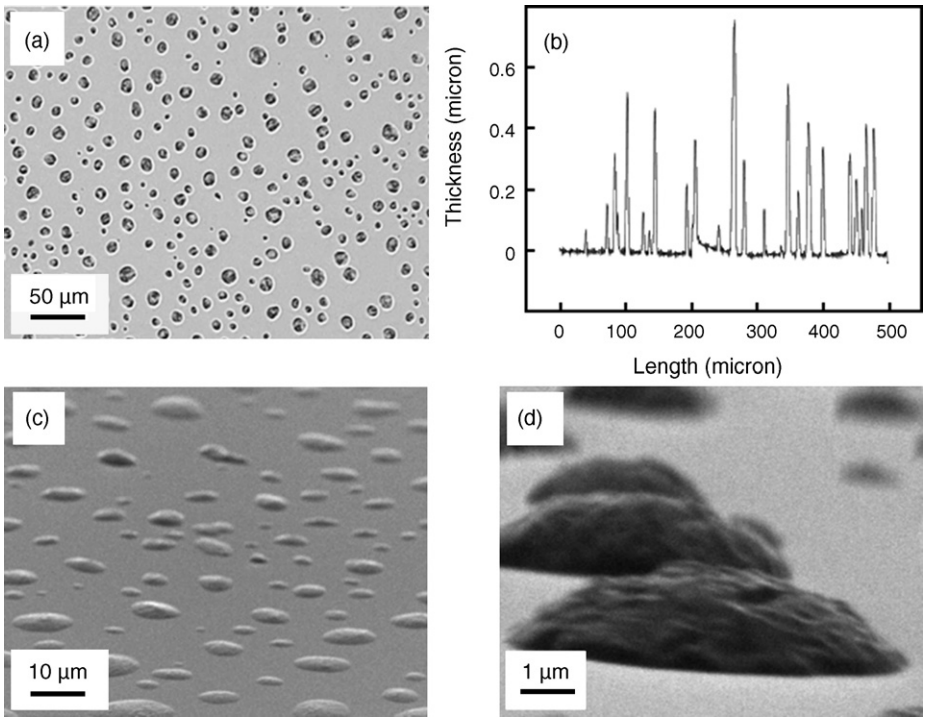

Fig. 2. (a) Optical microscope picture, (b) profilometer measurements and (c and d) SEM pictures of droplets obtained upon dewetting at 190–210 °C of a 50 nm thick film of Pe4C5 on untreated ITO substrates.

crystallization was observed, indicating that crystallization is strongly hindered in this confined geometry of a thin film. Upon heating, instabilities appeared below the clearing transition, in the liquid crystal phase, at about 190 °C, to form drop-shaped clusters on the surface (Fig. 2a). This phenomenon is fast (≈2 s) and the droplets remain approximately unchanged in shape upon further heating into the isotropic phase and after cooling down to room temperature. The drops are well-visible in the scanning electron microscopy (SEM) pictures in Fig. 2c and d. Contact angle measurements from SEM pictures indicate an average value of about 12°. The thickness of the drops is typically around 100 nm but can reach 400 nm (Fig. 2b) and planar orientation can be observed under crossed polarizers.

Our goal is to find chemical factors that affect the surface energy and to check whether these factors influence the wetting behavior of thin organic films. It has been shown on ITO that contact angles decrease [13] after specific surface treatments, but no changes in the wetting behavior of organic layers have been reported so far.

We have used five different methods for treating the ITO substrates:

(A) Immersion of the substrates in a caustic bath (1 mol/L NaOH) at 80 °C (30 min), followed by rinsing with deionized water and drying under nitrogen flow.
(B) Immersion of the substrates in a sulfochromic acid bath at 25 °C (30 min), followed by rinsing with deionized water and drying under nitrogen flow.
(C) DC argon plasma treatment (10 W, 150 s).
(D) UV–ozone treatment (150 s).
(E) Annealing at 500 °C in ambient atmosphere during 30 min.

No changes in roughness (<3 nm) were detected by AFM measurements after all the treatments.

Table 1 shows the surface energy after different ITO surface treatments, calculated from contact angles measured with water and diiodomethane. The equilibrium contact angle, θ, for a liquid drop on an ideal, homogeneous, planar and non-deformable surface is related to the interfacial tensions by Young's equation [14]:

$$\gamma_l \cos\theta = \gamma_s - \gamma_{sl} \quad (1)$$

Table 1
Contact angles and surface energies after different treatments

ITO treatments	Water contact angle (°)	Diiodomethane contact angle	Surface energy (mJ/m^2)	γ_s^p (mJ/m^2)	γ_s^d (mJ/m^2)
Methanol	62	40	55	17	38
NaOH	23	26	77	33	44
Sulfochromic acid	17	23	73	34	39
Argon plasma	4	31	81	38	43
UV–ozone	6	29	80	38	42
Annealing	4	29	81	38	43

Table 2
Elemental concentrations and ratios in the ITO surface as determined by XPS

Treatments	C	O	In	Sn	Na	In/Sn	O/In	C/In
Methanol	17.8	56.9	23.1	2.2	0.0	10.5	2.5	0.8
NaOH	14.3	50.6	26.0	2.4	6.8	10.8	1.9	0.5
Sulfochromicacid	9.8	59.9	27.5	2.7	0.0	10.2	2.2	0.3
Plasma	11.6	66.6	19.9	1.9	0.0	10.5	3.3	0.6
Annealing	11.6	60.4	25.5	2.4	0.0	10.6	2.4	0.4
UV–ozone	10.7	61.4	25.4	2.4	0.0	10.6	2.4	0.4

All the values are given in percentage.

where γ_l is the surface tension of the liquid in equilibrium with its saturated vapor, γ_s the surface tension of the solid in equilibrium with the saturated vapor of the liquid and γ_{sl} is the interfacial tension between the solid and the liquid.

According to Wu [15], the estimation of the solid–air energy was based on the following simplifying assumptions: (1) the total surface energies of the solid and liquids are the sum of their dispersion γ^d and polar γ^p surface energy components, (2) the solids and liquids interact only by means of dispersion and polar forces. Solid surface free energy can be assessed by contact angle measurements of two liquids of known polarity.

$$(1+\cos\theta)\gamma_l = \frac{4(\gamma_s^d \times \gamma_l^d)}{\gamma_s^d + \gamma_l^d} + \frac{4(\gamma_s^p \times \gamma_l^p)}{\gamma_s^p + \gamma_l^p} \quad (2)$$

where γ_l is the liquid surface tension and γ_s is the solid surface free energy.

We observe a surface energy increase after all the treatments as already published in the literature [16,17] (Table 1). The improvement of the polar component may indicate a substantial increase of OH species on the ITO surface.

3.1. XPS measurements

In order to analyze the chemical surface of the substrate, XPS measurements were carried out before and after the treatments. Table 2 shows the atomic concentrations of elements on the ITO surface. We observe a strong decrease in the carbon contamination after all the treatments. The most important variations occur after sulfochromic bath immersion. The NaOH bath induced the onset of sodium in the surface (6.8%), probably because rinsing with deionized water was not efficient in this case. The In/Sn ratio remains constant (about 10.5) after each treatment indicating that there is no selective etching. The O/In ratio shows stronger variations, especially after an argon plasma (increase) and a NaOH (decrease) treatment. We can conclude from these results that the observed modifications of the surface energy can be related to a large extent to the decrease in the surface carbon contamination and to an increase in oxygen bonding [13].

Analysis of the surface bondings is performed to relate the chemical state to the wetting process. Resolved peaks of indium, tin, oxygen and carbon of an untreated sample are indicated by full curves in Fig. 3. The difference between the experimental spectrum and the synthetic one is shown on the base line of the plot. The spectrum of indium (Fig. 3b) is located at 444.7 eV (5/2) and 452.4 eV (3/2), that of tin is peaked at 486.8 eV (5/2) 495.2 eV (3/2). These values agree with those reported by Ip et al. [18] and by Clark et al. [19]. We found that all the In $3d_{5/2}$ core-level spectra could be fitted with three Gaussian and Lorentzian functions of variable intensities centered at: 444.8 eV associated to In_2O_3, 446 eV attributed to indium hydroxide and 442.4 eV assignable to metallic indium [20]. The Sn $3d_{5/2}$ line (Fig. 3d) is composed of two peaks located at 486.9 and 488 eV, respectively. These components correspond to two different oxidation state of the tin atoms (Sn^{2+} and Sn^{4+}) [21].

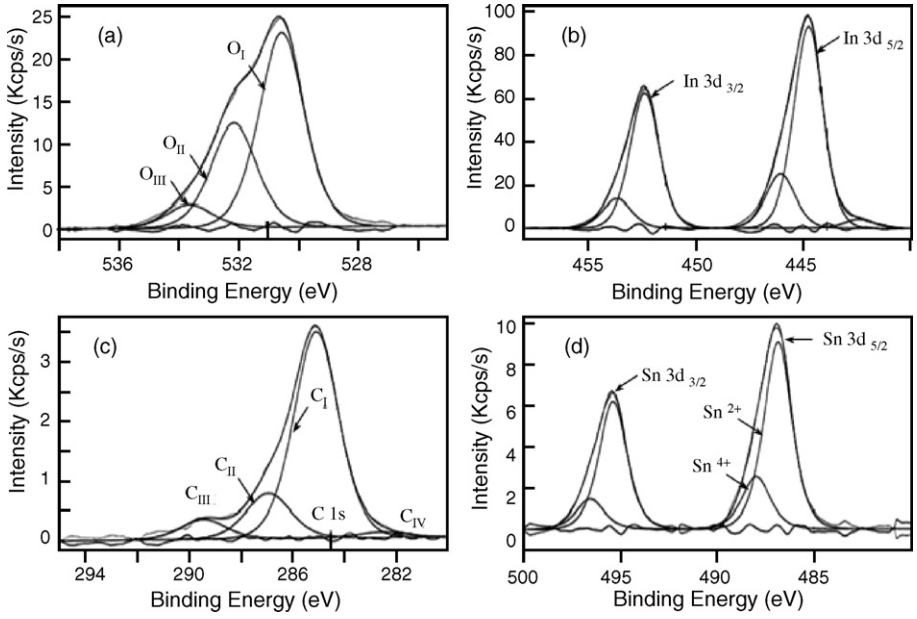

Fig. 3. Oxygen (a), indium (b), carbon (c) and tin (d) XPS spectra of untreated ITO surface.

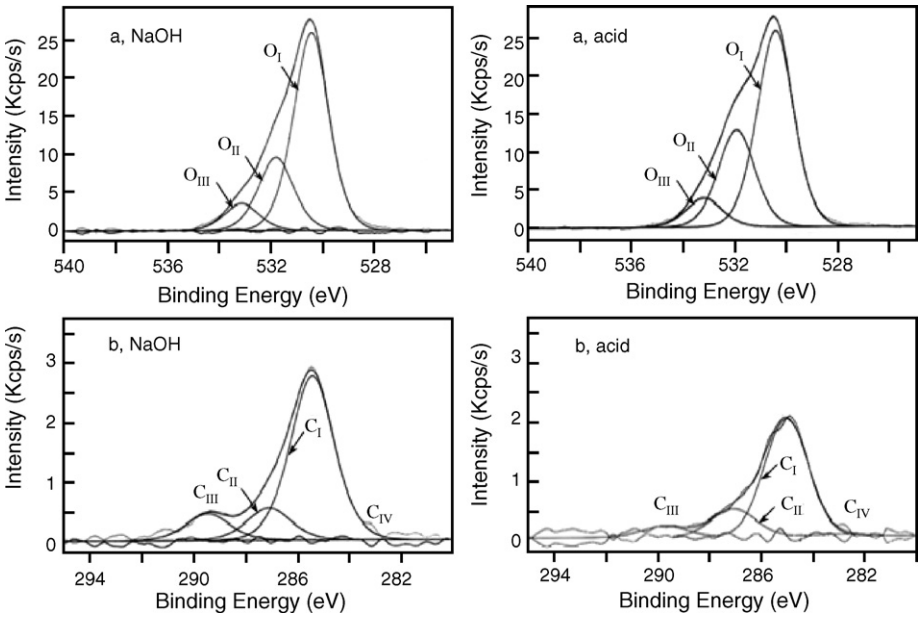

Fig. 4. Oxygen (a) and carbon (b) XPS spectra of NaOH and sulfochromic acid treated ITO surfaces.

The deconvoluted O 1s spectra (Fig. 3a) allow us to distinguish three peaks. One due to In_2O_3 is located at around 530.5 eV (referred to as O_I). The second one, around 532.5 eV (referred to as O_{II}), can have multiple sources, $In(OH)_3$, InOOH or O=C. The last one, centered at 533.6 eV (referred to as O_{III}), corresponds to O–C or H_2O adsorption.

The decomposition of the carbon spectrum (Fig. 3c) shows four components: the first component (C_I) is located at 285 eV and corresponds to carbon C–C/C–H, the second and the third ones ((C_{II} and C_{III}) to oxygen bonding in the form of C–O at 286.9 eV and C=O at 289.4 eV, respectively. The last peak (C_{IV}) is very weak and can be assigned to organometallic bonding.

The formation of indium hydroxide $In(OH)_3$ or InOOH can be attributed to the methanol cleaning and the deionized water rinsing. Water molecules are decomposed to form hydroxyl ions and protons and the OH^- radicals bind to the ITO forming hydroxide or oxy-hydroxide compounds [22–27]. Kim et al. calculated the rate between hydroxide and oxide forms by showing that the theoretical rate of oxygen in the ITO, O/(In + Sn), is equal to 1.5 if all the oxygen exists under O^{2-} form and 3 if all the oxygen is under OH^- form. In our case, $(O_I + O_{II})/(In + Sn)$ is equal to 2.1 [22]. Albeit the untreated substrate shows only oxygen of type O^{2-} bound to In^{3+} and Sn^{4+}, this calculation shows a rather significant quantity (about 40%) of $In(OH)_3$ (or InOOH).

The resolved spectra of ITO treated samples are displayed in Figs. 4–6. After NaOH treatment, the carbon spectrum shows a selective etching: the C_{III} peak corresponding to C=O bonding

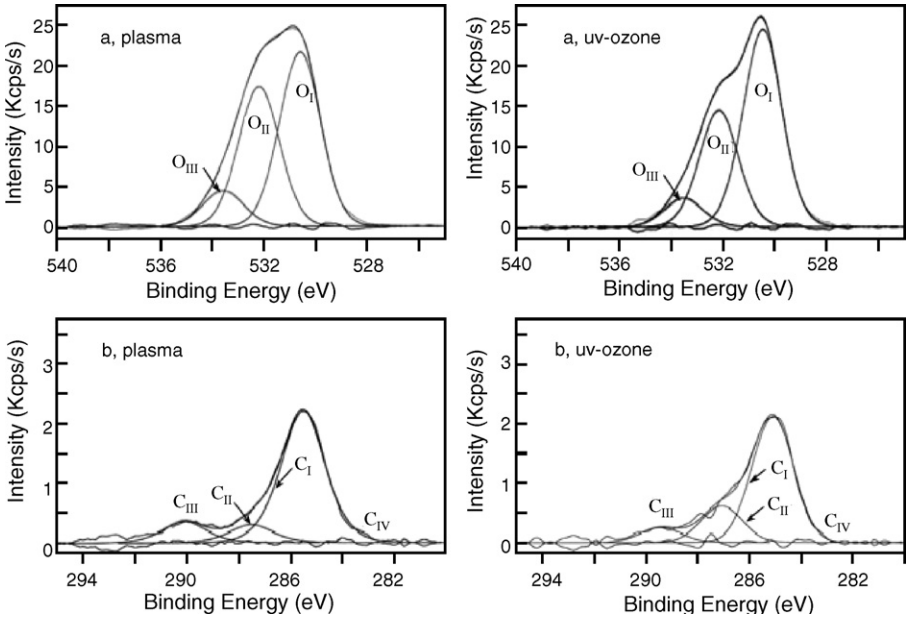

Fig. 5. Oxygen (a) and carbon (b) XPS spectra of argon plasma and UV–ozone treated ITO surfaces.

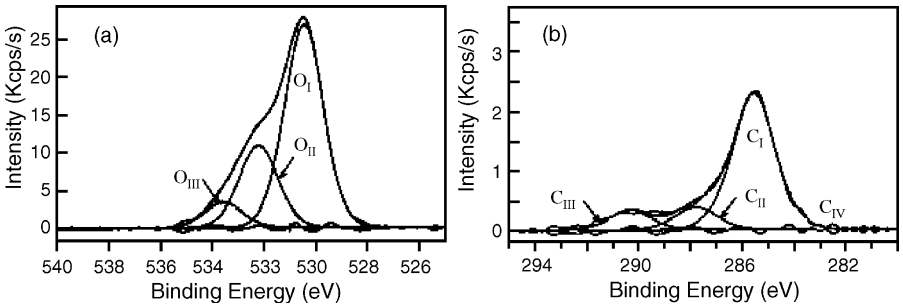

Fig. 6. Oxygen (a) and carbon (b) XPS spectra of annealed ITO surface.

increases in intensity after treatment. The second O_{II} component of the oxygen spectra and the first In_I peak of the indium spectra are also enhanced. The formation of O^{2-} is favored by the caustic bath. We note that the O_{III} peak intensity increases without variations of the C_{II} peak corresponding to C–O bonding. Thus, this oxygen peak enhancement can be related to the presence of H_2O on the ITO surface.

For acid sulfochromic treatment, the results in Fig. 4 show a large reduction of the carbon contamination without selective etching since all the resolved curves of the carbon spectra keep their proportions. As in the case of NaOH treatment, acid sulfochromic etching would promote formation of In_2O_3 and SnO_2 as show the oxygen, indium and tin spectra. Water adsorption is also detected by the increase of the O_{III} oxygen peak.

The carbon spectrum of the argon plasma treated ITO sample exhibits a large reduction in the carbon contamination but the etching is selective since the C_{III} peak, which is assigned to C=O bonding, is not reduced. On the other hand, the O_I oxygen intensity decreases strongly whereas O_{II} and O_{III} increase. This observation reveals the formation of hydroxide species and the presence of water on the ITO surface. However, we note that the indium spectrum does not show any corresponding variation. It can be therefore presumed that oxy-hydroxide species like InOOH have been formed resulting from the treatment of the sample.

UV–ozone is a powerful source that can be used to decrease the carbon contamination of the ITO surface. In Fig. 5, we observe that the C_{II} component of the carbon spectrum is slightly decreased suggesting that the etching of C–C and C=O bonding is selective. On the contrary, the treatment enhanced the O_{II} and O_{III} peaks indicating that hydroxide species are present. As in the case of the argon plasma treatment, we note that the In_{II} and Sn_{II} components decrease in intensity and we presume the creation of In–O–OH and Sn–O–OH bonding and water adsorption by the UV–ozone treatment.

Fig. 6 shows the oxygen and carbon spectra of the ITO surface after thermal annealing. We observe a large reduction of the carbon components except the component assigned to C=O. At the same time, the O_{II} oxygen component decreases and the variation can be observed also on the indium spectra with a reduction of the In_{II} component. The Sn spectrum shows a different situation with an increase of the Sn_{II} component. From this analysis, we suggest that annealing promotes formation of tin hydroxide SnOH and indium oxide In_2O_3. The O_{III} oxygen peak does not show any variation in spite of the carbon reduction, it can be therefore related to the presence of H_2O on the ITO surface.

XPS analysis was also used to analyze very thin films of the perylene derivative on the substrate in order to check if new chemical species were created at the ITO/organic interface. For this purpose, a 5 nm perylene derivative film was deposited on all substrates (treated and untreated). The oxygen and carbon peaks were modified by the presence of the organic molecules and correspond to the reference spectra of perylene derivative. Indium and tin peaks were also present and did not show any changes in their proportions as compared to uncoated ITO substrates. All the changes in the XPS spectra induced by the different treatments were still visible after deposition of the perylene derivative film. Moreover, when depositing a 10 nm thick film of perylene derivative on the ITO substrate, an indium peak could still be detected on the surface of the organic film. Thus, no chemical reaction between ITO and perylene derivative could be observed, but indium had diffused into the organic thin film [20].

3.2. Wetting observations

During the annealing of a 50 nm thick film on treated ITO, different behaviors were observed with different ITO treatments and different film thicknesses.

Firstly, caustic soda and sulfochromic acid treated surfaces do not suppress dewetting below the clearing transition, but the effect is less important than that obtained in non-treated substrates. No film thickness dependence of the dewetting was observed for these treatments.

Samples treated by argon plasma, UV–ozone and annealing exhibit very similar behavior, that is, no significant morphology difference could be observed by optical microscopy between these three treatments, and the wetting behavior was significantly improved. While very thin films of less than 40 nm thickness still dewet once the isotropic phase is reached, films of 50 nm thickness dewet only partially around discrete nucleation centers. For thicknesses above 100 nm, the film is stable in the isotropic phase except for some rare and small dewetted spots (Fig. 7).

Films that are thick enough (>40 nm) to wet the surface in the isotropic phase can exhibit another dewetting phenomenon when cooled through the isotropic to LC phase transition. The growth of liquid crystalline domains is accompanied by

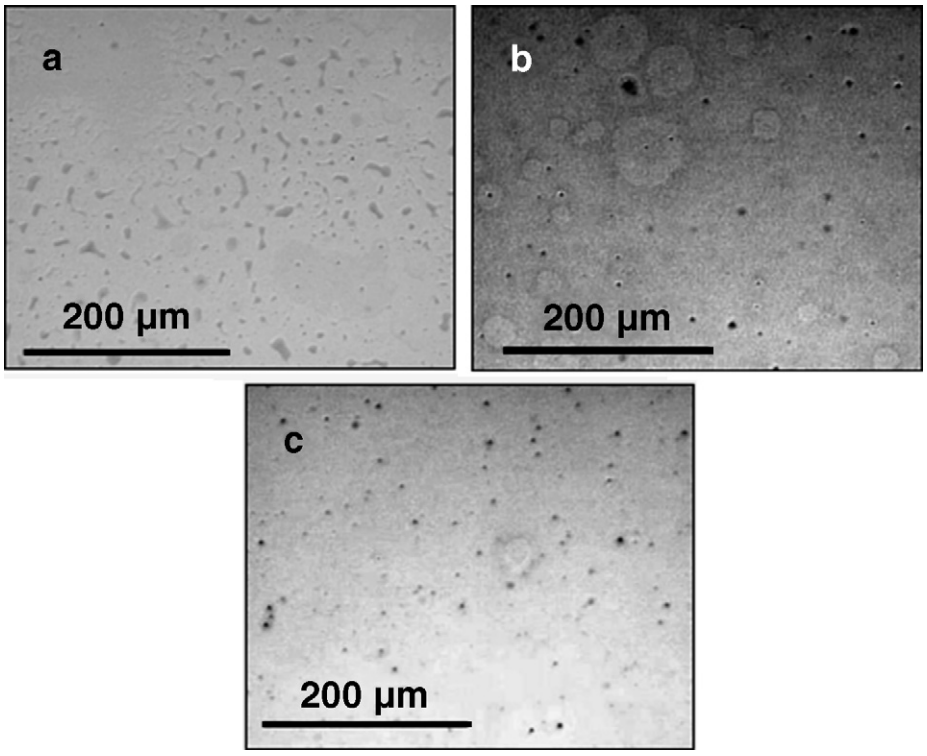

Fig. 7. (a) 20 nm, (b) 50 nm and (c) 100 nm thin film of Pe4C5 after 15 min in the liquid phase on argon plasma treated ITO surface.

dewetting in the areas around them (Fig. 8). This phenomenon is dependent on the cooling rate and can be suppressed by a rapid cooling down to temperatures much lower than the phase transition (Fig. 9) [10].

4. Discussion

The XPS results demonstrate the carbon decontamination and the generation of In–OH (or In–O–OH), Sn–OH (or Sn–O–OH) bonding and water adsorption on ITO surface before and after treatments. These changes could be quantified by the analysis of oxygen peaks as shown previously. The calculated percentage of hydroxyl ions and atomic carbon concentration recorded after each treatment are summarized in Table 3. At first glance, one can note that the modifications of the wetting properties are related to a large extent to the decrease of the surface carbon contamination: samples show less dewetting with any treatment than without. Hydrophobic bonds, In–O–In or Sn–O–Sn, are partially replaced by hydrophilic groups In–OH and Sn–OH (or In–O–OH) on the ITO surface. These polar

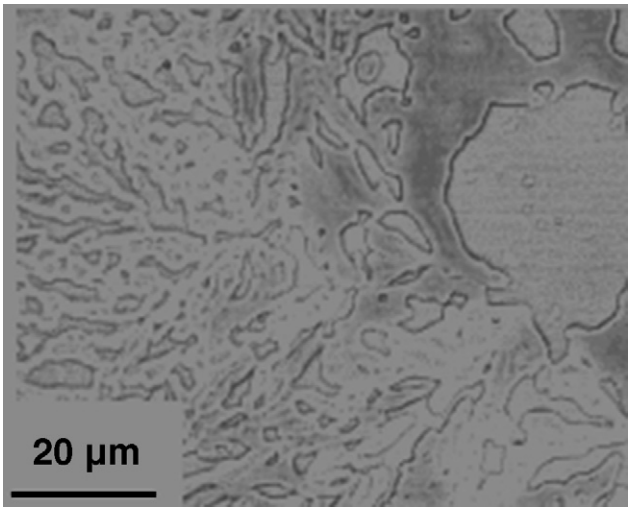

Fig. 8. Phase transition induced dewetting of a 100 nm thick film of Pe4C5 upon growth of LC domains during slow cooling on argon plasma treated ITO surface observed by optical bright field microscopy.

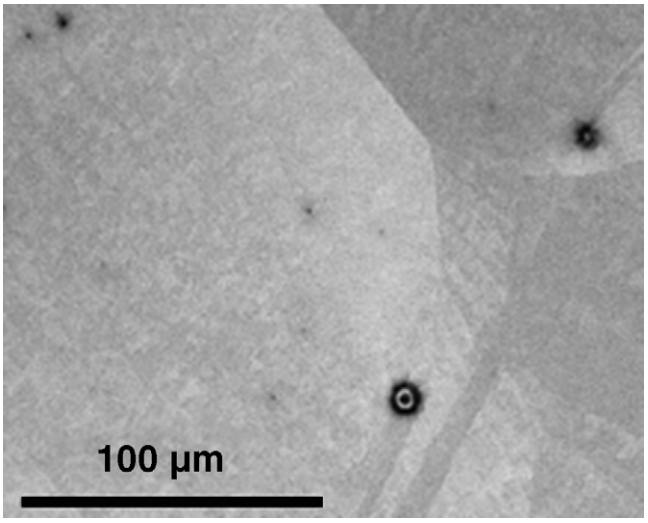

Fig. 9. One hundred nanometers thick film of Pe4C5 after fast cooling (by removal from the oven in the isotropic state) on argon plasma treated ITO surface seen by optical bright field microscopy. No dewetting is observed.

Table 3
Hydroxydes and atomic carbon concentration in ITO substrates treated with different processes

Treatments	OH^-	C
Untreated	40	17.8
Caustic	10	14.3
Acid	18	9.8
Plasma	83	11.6
Annealed	33	11.6
Ozone	33	10.7

All the values are given in percentage.

species greatly improve the surface energy and can be considered to be the second prevailing factor influencing the wetting properties.

In the case of an untreated substrate, in spite of a high hydroxide concentration (about 40% due to methanol cleaning) the carbon contamination is too high and the Pe4C5 layer dewet. After an acid or a caustic treatment, the carbon concentration decreased but a small quantity of hydroxide species was retrieved: the wetting was improved but not as much as the last three treatments; argon plasma, annealing and UV–ozone. The latter exhibited a low carbon contamination and a superior hydroxide concentration, above 30%. These two parameters lead to a spectacular enhancement of the wetting properties as shown previously.

In the XPS analysis, we assigned the observed O_{III} component of O 1s spectra to O–C and/or H_2O. However, the variation of this component in the XPS spectra of treated samples is not in accordance that of the C_{III} component of the carbon spectra. Therefore, a water adsorption layer on the ITO surface has likely formed, resulting from the applied treatment process. The methanol cleaning and deionized water rinsing may at the origin of this contamination and the formation of a high energy polar surface would contribute to attract H_2O molecules. The polar species – water, hydroxides and oxy-hydroxides – improve the surface energy and then reduce the Pe4C5 layer dewetting.

Instabilities can occur in thin films when Van der Waals forces induce attractive potential between the two interfaces (ITO/Pe4C5 and Pe4C5/air). This effective interface potential $P(h)$, between the two interfaces separated by a distance h can be written as:

$$P(h) = -\frac{A}{12\pi h^2} \tag{3}$$

A is related to the Hamaker constant. This equation does not take into account short range forces that make P tend to a constant value when h tends towards 0. The approximate expression proposed by Israelachvili for the non-retarded Hamaker constant for two macroscopic phases 1 and 2 interacting across a medium 3 is the following:

$$A = \frac{3}{4}kT\left(\frac{\varepsilon_1-\varepsilon_3}{\varepsilon_1+\varepsilon_3}\right)\left(\frac{\varepsilon_2-\varepsilon_3}{\varepsilon_2+\varepsilon_3}\right) + \frac{3h\nu_e}{8\sqrt{2}} \times \frac{(n_1^2-n_3^2)(n_2^2-n_3^2)}{\sqrt{(n_1^2+n_3^2)(n_2^2+n_3^2)}\left(\sqrt{n_1^2+n_3^2}+\sqrt{n_2^2+n_3^2}\right)} \tag{4}$$

where ν_e is the main electronic absorption frequency in the UV, typically around $3 \times 10^{15}\ s^{-1}$. n_1, n_2, n_3 and ε_1, ε_2, ε_3 are, respectively, the refractive index and the dielectric constant of the three materials ITO/Pe4C5/air [28]. The second term, related to the dispersive energy component, is dominant in this system because the dielectric constants are low. The Hamaker constant is negative assuming refractive indices of 2 for ITO and 1.6 for Pe4C5 and dielectric constants of 9 for ITO and 2.7 for Pe4C5. According to Eq. (1), $P(h)$ is then positive, i.e., interfacial forces are repulsive and tend to thicken the film, hence no instabilities occur.

If we take account of a thin film of water (thickness, l) detected by XPS analysis on the ITO surface, the effective interface potential can be written as a function of the organic material thickness, h:

$$P(h) = -\frac{A_{H_2O}}{12\pi h^2} + \frac{A_{H_2O}-A_{ITO}}{12\pi(h+l)^2} \tag{5}$$

A_{H_2O} is the related Hamaker constant of the system H_2O/Pe4C5/air with the refractive index and the dielectric constant of water as $n = 1.33$ and $\varepsilon = 80$, respectively [30–33]. Fig. 10 shows the variation of P as a function of the organic layer thickness l, with and without a thin water layer of thickness

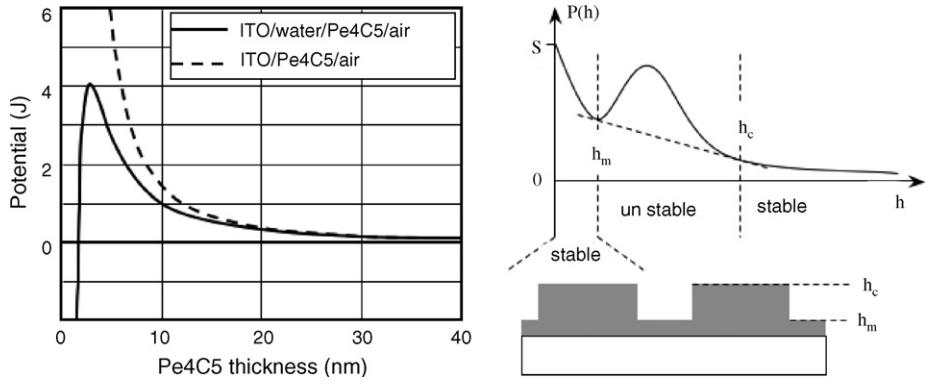

Fig. 10. Calculated effective interface potential function to the Pe4C5 thickness (left) and theoretical potential (right) with pseudo-partial wetting situation, two thicknesses are in coexistence.

$h = 1$ nm. The positive value of P for the system without water indicates a stable regime over the entire thickness range. If we take account of an adsorption of water on the ITO substrate, the stability of the organic layer is modified and is a function of the thickness of the organic layer. The intensity of the destabilizing effect can be modulated by the coupling value of P when h tends towards 0. Thus, after argon plasma, UV–ozone and annealing treatments of ITO surface in our case, $P(h)$ could have the behavior shown in Fig. 10.

The existence of a minimum value for P suggests the existence of a stable zone if the initial film thickness is inferior to h_m. If the thickness of the organic layer is superior to h_m, the system is in a pseudo-partial wetting state: a very thin film, of thickness h_m, is still present between the drops. In this case, the film is composed of different zones having two different thicknesses (Fig. 10) [29]. When $h > h_c$ the wetting is complete. The dependence of dewetting on organic layer thickness can be related to this pseudo-partial wetting phenomenon with a value of h_c close to 40 nm and a very small value of h_m (0–5 nm). Note that this nanometric film cannot be seen by optical microscopy. Our XPS measurements suggest that this mechanism could be induced by water adsorption and other polar species. This situation can be compared to the dewetting of polystyrene (PS) films on Si substrate covered by a native oxide. Different situations of wetting were observed as a function of the thickness of the oxide and the PS [31,32]. As in our case, the dispersive energy component in the Hamaker constant drives the system because the dielectric constants are weak. Then, if the refractive index of the surface layer that has formed on the substrate is smaller than that of the organic thin film, dewetting will occur. The thicker the surface layer, the more pronounced is the destabilizing effect. Moreover, Sarlah and Zumer demonstrate the possibility of a significant change in the Van der Waals interaction in the case of a nematic liquid crystal formed on solid surfaces due to a thin layer of water [30].

5. Conclusion

The dewetting of thin films of a discotic liquid crystal on a solid surface can be prevented by modifying the substrate, combined with fast cooling through the isotropic-to-LC transition. We have performed different ITO treatments to improve the ITO surface energy. Argon plasma, annealing and UV–ozone treatments induced good wetting conditions to obtain a homogeneous organic thin film. Contact angle measurements confirmed the improvement in the substrate surface energy. XPS was used to identify the chemical nature of the ITO surface. The reduction in the carbon contamination and the presence of polar species like $In_2(OH)_3$ and H_2O were thus demonstrated. These two factors are necessary to obtain a large surface energy and greatly influence the dewetting process. The formation of these polar species and the adsorption of water lead to a pseudo-partial wetting situation as a function of the organic layer thickness. The study of the dewetting behavior of columnar liquid crystalline films as a function of its alignment is currently under way.

References

[1] S.H. Kim, Y.S. Yang, J.H. Lee, J. Lee, H.Y. Chu, H. Lee, J. Oh, L. Do, T. Zyung, Opt. Mater. 21 (2002) 439.
[2] C.E. Lee, J.W. Jang, H.M. Lee, D.K. Oh, C.H. Lee, D.W. Lee, J. Jin, Curr. Appl. Phys. 1 (2001) 107.
[3] H. Yanagi, Y. Araki, T. Ohara, S. Hotta, M. Ichikawa, Y. Taniguchi, Adv. Funct. Mater. 13 (2003) 767.
[4] F. Yang, M. Shtein, S.R. Forrest, Nat. Mater. 4 (2005) 37.
[5] A.M. van de Craats, J.M. Warman, A. Fechtenkötter, J.D. Brand, M.A. Harbison, K. Müllen, Adv. Mater. 11 (1999) 1469.
[6] L. Schmidt-Mende, A. Fechtenkötter, K. Müllen, R.H. Friend, J.D. MacKenzie, Phys. E 14 (2002) 263.
[7] K. Petritsch, R.H. Friend, A. Lux, G. Rozenberg, S.C. Moratti, A.B. Holmes, Synth. Met. 102 (1999) 1776.
[8] B. Kippelen, S. Yo, B. Domercq, C.L. Donley, C. Carter, W. Xia, B.A. Minch, D.F. O'Brien, N.R. Armstrong, NCPV and Solar Program Review Meeting, Denver, 21–23 March, 2003, p. 431.
[9] M. Oukachmih, P. Destruel, I. Séguy, G. Ablart, P. Jolinat, S. Archambeau, M. Mabiala, S. Fouet, H. Bock, Sol. Energy Mater. Sol. Cells 85 (2005) 535.
[10] E. Grelet, H. Bock, Europhys. Lett. 73 (2006) 712.
[11] I. Séguy, P. Jolinat, P. Destruel, J. Farenc, R. Mamy, H. Bock, J. Ip, T.P. Nguyen, J. Appl. Phys. 89 (2001) 5442.
[12] T. Hassheider, S.A. Benning, H.S. Kitzerow, M.F. Achard, H. Bock, Angew. Chem. 113 (2001) 2119.
[13] J.S. Kim, R.H. Friend, F. Cacialli, Synth. Met. 111–112 (2000) 369.
[14] P.G. de Gennes, F. Brochard-Wyart, D. Quere, Gouttes, Bulles, Perles et Ondes, Belin, Paris, Collection Echelles, 2002.
[15] S. Wu, Polymer Interface and Adhesion, Marcel Dekker, New York, 1982
[16] Z. Zhong, et al. Phys. Status Solidi A 198 (2003) 197.
[17] H. Kim, J. Lee, C. Park, Y. Park, J. Korean Phys. Soc. 41 (2002) 39.
[18] J. Ip, T.P. Nguyen, P. Le Rendu, Synth. Met. 138 (2003) 107.
[19] D.T. Clark, T. Fox, G.G. Roberts, R.W. Sykes, Thin Solid Films 70 (1980) 261.
[20] T.P. Nguyen, P. Le Rendu, S.A. de Vos, Synth. Met. 138 (2003) 113.
[21] H.Y. Yu, X.D. Feng, D. Grozea, Z.H. Lu, R.N.S. Sodhi, A.M. Hor, H. Aziz, Appl. Phys. Lett. 78 (2001) 2595.
[22] J.S. Kim, P.K.H. Ho, D.S. Thomas, R.H. Friend, F. Cacialli, G.W. Bao, S.F.Y. Li, Chem. Phys. Lett. 315 (1999) 307.
[23] J.S. Kim, F. Cacialli, M. Granström, R.H. Friend, N. Johansson, W.R. Salaneck, R. Daik, W.J. Feast, Synth. Met. 101 (2000) 111.
[24] J.A. Chaney, P.E. Pehrsson, Appl. Surf. Sci. 180 (2001) 214.
[25] J.A. Chaney, S.E. Koh, C.S. Dulcey, P.E. Pehrsson, Appl. Surf. Sci. 218 (2003) 259.
[26] K.X. Ma, C.H. Ho, F. Zhu, T.S. Chung, Thin Solid Films 371 (2000) 140.
[27] C. Donley, D. Dunphy, D. Paine, C. Carter, K. Nebesny, P. Lee, D. Alooway, N.R. Armstrong, Langmuir 18 (2002) 450.
[28] J. Israelachvili, Intermolecular and Surface Forces, second ed., Academic Press, New York/London, 1992.
[29] G. Reiter, A. Sharma, A. Casoli, M.O. David, R. Khanna, P. Auroy, Langmuir 1 (1999) 2551.
[30] A. Sarlah, S. Zumer, CNLS 21st Annual International Conference on the Principles of Soft Matter, Santa Fe, May 21–25, 2001.
[31] R. Seemann, S. Hermingaus, K. Jacobs, J. Phys. C: Condens. Matter 13 (2001) 4925.
[32] R. Seemann, S. Herminghaus, C. Neto, S. Schlagowski, D. Podzimek, R. Konrad, H. Mantz, K. Jacobs, J. Phys. C: Condens. Matter 17 (2005) 267.
[33] A. Sarlah, P. Ziherl, S. Zumer, Mol. Cryst. Liq. Cryst. 364 (2001) 443.